J|A|C|S COMMUNICATIONS

Published on Web 09/16/2009

Biomimetic Conformation-Specific Assembly of Proteins at Artificial Binding Sites Nanopatterned on Silicon

Roberto de la Rica* and Hiroshi Matsui*

Department of Chemistry and Biochemistry, City University of New York, Hunter College, 695 Park Avenue, New York, New York 10065

Received July 16, 2009; E-mail: hmatsui@hunter.cuny.edu; roberto.delarica@gmail.com

Biomolecules such as nucleic acids, enzymes, and antibodies have evolved the ability to recognize target molecules, a key factor in the origin of life.[1] These biomolecules possess binding sites where the molecular architecture and the physicochemical properties are optimum for their interaction with a particular target, in some cases even differentiating between stereoisomers. This exquisite specificity via the creation of a suitable chemical environment has inspired scientists to design new materials with the biomimetic recognition capability for its application in sensing[2] and catalysis.[3] In the present work, we recreate the conformation-specific interaction between calmodulin (CaM) and its natural receptors by tailoring the physicochemical properties of silicon in the sub-10 nm range via well-known surface chemical modification methodologies and nanolithography. While in the absence of Ca^{2+} the two helices of each helix−loop−helix unit of CaM run almost antiparallel to each other (apo-CaM, upper left in Figure 1), in the presence of Ca^{2+} these EF-hand motifs are perpendicular to each other, thus resulting in a dumbbell shape of the protein with an exposed hydrophobic central helix (Ca^{2+}−CaM, upper right in Figure 1).[4] Many CaM-binding domains present an amphiphilic structure, where hydrophobic residues interact with the exposed hydrophobic surface of Ca^{2+}−CaM and charged residues can make specific salt bridges with the acidic residues of the protein.[5] Therefore, an artificial nanostructure containing a hydrophobic core flanked by charged, hydrophilic domains could mimic the biological interaction between CaM and its targets, and hence it could discriminate between the two conformers of the protein.

To create biomimetic binding sites for Ca^{2+}−CaM, thermally oxidized silicon wafers were first modified with hydrophobic octyltrimethoxysilane (OTMS) molecules, and then covered with a layer of hydrophilic bovine serum albumin (BSA) (details available in the Supporting Information). Subsequently, BSA was removed at specific sites with the tip of an atomic force microscope (AFM). By this nanoshaving approach,[6] trenches consisting in a hydrophobic core (OTMS) surrounded by hydrophilic BSA molecules were obtained (Figure 1, down), thus providing amphiphilic cavities similar to the natural receptors of Ca^{2+}−CaM. In Figure 2a, three lines of 2 μm length separated by 200 nm were patterned with the contact mode of the AFM (force $\approx$ 10 nN, velocity $\approx$ 500 nm/s). By measuring 10 random height profiles along the pattern in the AC mode, the full-width-at-half-maximum (fwhm) of the trench was 10 ± 1 nm, thus making these structures one of the narrowest silane patterns ever achieved.[7−9] Then, this patterned substrate was incubated in a solution containing Ca^{2+}−CaM (a complete scheme of calmodulin binding in nanopatterns and posterior treatments is available as Figure S3, Supporting Information), and the presence of the protein on the OTMS lines was confirmed with an antibody that could target both the native and denatured forms of CaM,[10] and therefore did not show any selectivity for a particular conformer (see also Figure S6, Supporting Information). BSA was incubated before incubating anti-CaM because without this treatment the antibody could adsorb at defect sites of the BSA layer and degrade the precision of the protein assembly on the patterns. After incubation with anti-CaM, the average height of the hydrophobic lines incubated with Ca^{2+}−CaM increased from -0.5 ± 0.1 nm to 4.5 ± 0.8 nm ($n = 10$) as shown in Figure 2b, which indicated the binding of Ca^{2+}−CaM only on the nanopatterns. In contrast, the substrates in the apo-CaM solution did not show significant topographical change (Figure 2c) and the height profiles only represented the roughness of the surface, which indicated that they were filled up by BSA molecules in the blocking step rather than by apo-CaM. It should be noted that BSA could interact nonspecifically with the biomimetic binding sites during this blocking step because it was 10^5 times more concentrated than the target analyte. Moreover, Ca^{2+}−CaM could be removed from the patterns by washing the substrate with a Ca^{2+}-chelating agent, EGTA (Figure S5, Supporting Information), thus indicating that the binding of CaM was reversible and dependent only on the concentration of Ca^{2+} as it is observed in cells.

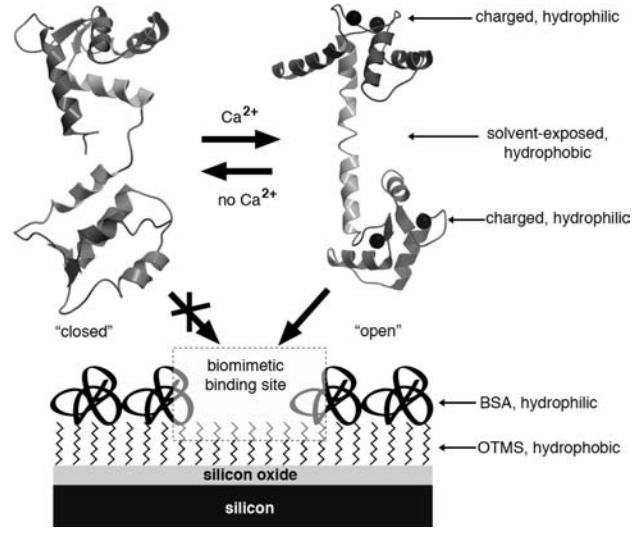

Figure 1. Schematic representation of the three-dimensional structures of Ca^{2+}-free CaM (apo-CaM, closed conformation, 3CLN) and Ca^{2+}−CaM (open conformation, 1DMO) and the biomimetic binding site. The black spheres represent calcium ions bound to carboxylic acid groups. The figure was prepared using ICM Molsoft 3.6−1.

In the natural binding sites, the dimension of the binding domains plays an important role in the creation of the suitable physicochemical environment for the specific recognition of the target. Similarly, we hypothesize that the width of the artificial binding sites is important and it needs to be tuned close to the size of CaM in the open conformation for the biomimetic recognition of Ca^{2+}−CaM. To examine this hypothesis, we fabricated wider

 10.1021/ja905932e CCC: $40.75

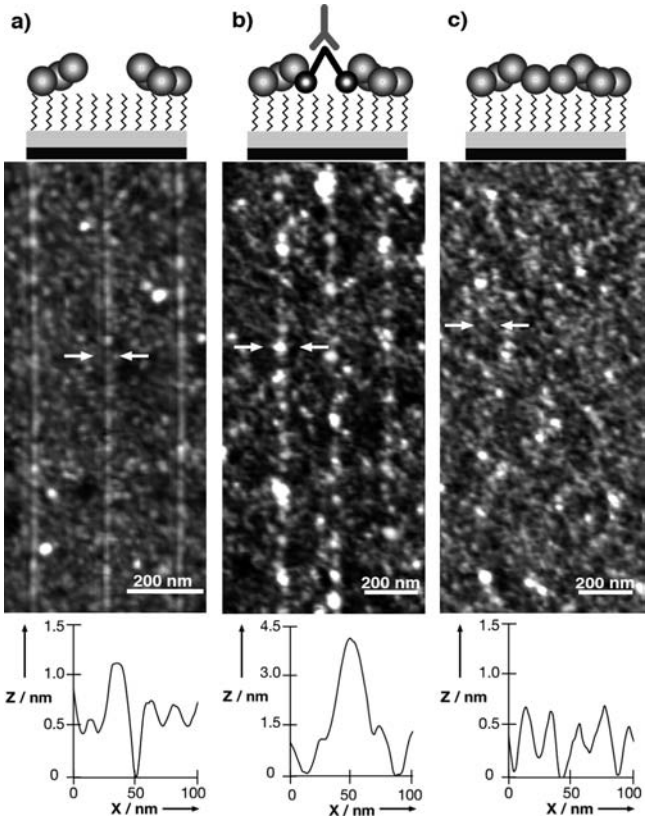

Figure 2. AFM images (topography) and height profiles (between arrows) of (a) binding sites as lines on silicon after performing the nanoshaving step, (b) the binding sites in (a) after incubation with Ca^{2+}−CaM and anti-CaM, (c) the binding sites in (a) after incubation with Ca^{2+}-free CaM and anti-CaM.

patterns of hydrophobic trenches on silicon substrates and incubated Ca^{2+}−CaM and apo-CaM, respectively. As the trench width was increased from 10 ± 1 nm to 17 ± 4 nm, both conformers were adsorbed in the trenches (Figure S4, Supporting Information), thus indicating that the dimensions of the biomimetic cavity are crucial for the specific recognition of Ca^{2+}−CaM. Since large hydrophobic surfaces could partially denature globular proteins to expose their hydrophobic core,[11] the wider hydrophobic trenches could induce a conformational change of apo-CaM to expose hydrophobic domains, which allows this conformer to bind the trench in a similar fashion as Ca^{2+}−CaM does (Figure S3, Supporting Information). In contrast, the narrower trenches have a smaller hydrophobic surface area, and therefore they have less impact on the denaturing of apo-CaM. Herein, the exposed central helix of Ca^{2+}−CaM can interact more favorably with the alkyl chains of OTMS and the charged residues of the two peripheral globular domains interact electrostatically with the BSA molecules, thus mimicking the biological interactions between Ca^{2+}−CaM and its natural receptors.

To further confirm our hypothesis, the location of anti-CaM bound to CaM patterns was imaged with a fluorescence microscope. After incubating a substrate containing 20 lines of 10 nm width, 2 μm length and 50 nm pitch with Ca^{2+}−CaM and anti-CaM, the anti-CaM was labeled with a secondary dye-conjugated antibody. The fluorescence image in Figure 3a shows the resulting 2 μm × 1 μm square pattern, which corresponds to the entire patterned area that contains all lines. Although the individual lines could not be resolved due to the limit of resolution of the microscope, this result confirmed that the biomimetic binding sites could recognize the

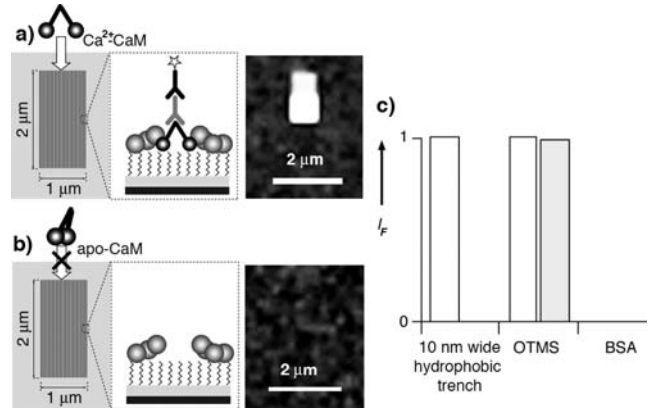

Figure 3. Fluorescence analysis of biomimetic binding sites and nonpatterned substrates; (a) binding sites after incubation with Ca^{2+}−CaM and immunoassay, (b) binding sites after incubation with apo-CaM and immunoassay, and (c) relative fluorescence intensity (I_F) of the patterned trenches, the OTMS-modified silicon surface, and the BSA-modified silicon surface. White bars, Ca^{2+}−CaM; gray bars, apo-CaM.

Ca^{2+}−CaM conformer. When the same experiment was repeated with apo-CaM, no fluorescence signal was observed in the region of interest (Figure 3b), thus demonstrating the selectivity of the hydrophobic patterns toward Ca^{2+}−CaM. The comparison of fluorescence intensity on each substrate is summarized in Figure 3c (see also Figure S6, Supporting Information). This bar graph shows that only Ca^{2+}−CaM binds hydrophobic trenches (10 nm × 2 μm) while both Ca^{2+}−CaM and apo-CaM nonspecifically attach to the OTMS-modified substrates, which is consistent with the AFM images in Figure 2. The BSA layer did not bind any CaM proteins, which confirmed the function of BSA as a stable mask in the fabrication and recognition process.

In summary, we recreated the conformation-specific recognition of CaM on silicon by downscaling well-known physicochemical phenomena in the sub-10 nm range. The concept could be adapted to mimic other interactions for sensing and catalysis by using silanes with different functionalities and/or different protein layers.

Acknowledgment. This work was supported by the U.S. Department of Energy (DE-FG-02-01ER45935). Hunter College infrastructure is supported by the National Institutes of Health, the RCMI program (G12-RR003037-245476). R.R. acknowledges a postdoctoral fellowship from the Spanish Ministerio de Ciencia e Innovación and Fundación Española para la Ciencia y la Tecnología

Supporting Information Available: Fabrication of biomimetic binding sites (Figure S1), Figures S2−S6, Experimental details. This material is available free of charge via the Internet at http://pubs.acs.org.

References

(1) Bada, J. L.; Lazcano, A *Science* **2002**, *296*, 1982–1983.
(2) Holthoff, E. L.; Bright, F. V. *Acc. Chem. Res.* **2007**, *40*, 756–767.
(3) Ramstrom, O.; Mosbach, K. *Curr. Opin. Chem. Biol.* **1999**, *3*, 759–764.
(4) Zhang, M. J.; Yuan, T. *Biochem. Cell Biol.* **1998**, *76*, 313–323.
(5) Ikura, M.; Clore, G. M.; Gronenborn, A. M.; Zhu, G.; Klee, C. B.; Bax, A. *Science* **1992**, *256*, 632–638.
(6) Shi, J.; Chen, J.; Cremer, P. S. *J. Am. Chem. Soc.* **2008**, *130*, 2718–2719.
(7) de la Rica, R.; Baldi, A.; Mendoza, E.; Paulo, A. S.; Llobera, A.; Fernandez-Sanchez, C. *Small* **2008**, *4*, 1076–1079.
(8) Pallandre, A.; Glinel, K.; Jonas, A. M.; Nysten, B. *Nano Lett.* **2004**, *4*, 365–371.
(9) Ivanisevic, A.; Mirkin, C. A. *J. Am. Chem. Soc.* **2001**, *123*, 7887–7889.
(10) Hulen, D.; Baron, A.; Salisbury, J.; Clarke, M. *Cell Motil. Cyto.* **1991**, *18*, 113–122.
(11) Kim, J.; Somorjai, G. A. *J. Am. Chem. Soc.* **2003**, *125*, 3150–3158.

JA905932E